(8) Dack, R. J. In *Techniques of Chemistry* (*Solutions and Solubilities*); Weissberger, Ed.; Wiley: New York, 1975; Vol. 8, pp 412-413.
(9) López, M. C.; Gallardo, M. A.; Urieta, J. S.; Gutiérrez Losa, C. *Rev. Acad. Cienc. Exactus, Fis. Quim. Nat. Zaragoza* **1988**, *43*, 183.
(10) López, M. C.; Gallardo, M. A.; Urieta, J. S.; Gutiérrez Losa, C. *Rev. Acad. Cienc. Exactus, Fis. Quim. Nat. Zaragoza* **1988**, *43*, 191.
(11) Brückl, N.; Kim, J. *Z. Phys. Chem.* (*Munich*) **1981**, *126*, 133.
(12) McClelland, A. L. *Tables of Experimental Dipole Moments*; Freeman: San Fransisco, 1963; pp 123-124.
(13) Wilhelm, E.; Battino, E. *J. Chem. Phys.* **1971**, *55*, 4012.
(14) Wilhelm, E. *J. Chem. Phys.* **1973**, *58*, 3358.
(15) Wilhelm, E.; Battino, E. *J. Chem. Thermodyn.* **1971**, *3*, 379.
(16) Pierotti, R. A. *Chem. Rev.* **1976**, *76*, 717.
(17) Reiss, H.; Frisch, E.; Helfand, E.; Lebowitz, J. L. *J. Chim. Phys. Phys.-Chim. Biol.* **1960**, *32*, 119.
(18) Gallardo, M. A.; Urieta, J. S.; Gutiérrez Losa, C. *J. Chim. Phys. Phys.-Chim. Biol.* **1983**, *80*, 718.
(19) Byrne, J. E.; Battino, R.; Wilhelm, E. *J. Chem. Thermodyn.* **1975**, *7*, 715.
(20) Wilcock, R. J.; Battino, R.; Wilhelm, E. *J. Chem. Thermodyn.* **1977**, *9*, 111.

Received for review March 10, 1989. Accepted September 12, 1989. We are grateful to the Comision Asesora de Investigación Cientifica y Técnica (Madrid) for financial assistance (Proyecto 1977/82).

Isothermal Vapor–Liquid Equilibrium Data for Binary Systems at High Pressures: Carbon Dioxide–Methanol, Carbon Dioxide–Ethanol, Carbon Dioxide–1-Propanol, Methane–Ethanol, Methane–1-Propanol, Ethane–Ethanol, and Ethane–1-Propanol Systems

Kazuhiko Suzuki* and Haruhusa Sue
Central Research Laboratories, Idemitsu Kosan Company, Ltd., Sodegaura, Chiba 299-02, Japan

Masahiro Itou, Richard L. Smith, Hiroshi Inomata, Kunio Arai, and Shozaburo Saito
Department of Chemical Engineering, Tohoku University, Sendai 980, Japan

Isothermal vapor–liquid equilibrium data for binary systems carbon dioxide–methanol, carbon dioxide–ethanol, carbon dioxide–1-propanol, methane–ethanol, methane–1-propanol, ethane–ethanol, and ethane–1-propanol were measured by a new static phase equilibrium apparatus at 313.4 and 333.4 K.

Introduction

Production of C_1 to C_6 alcohols from syngas is one of the most promising developments in C_1 chemistry. The reactions are

main reactions

$$n\mathrm{CO} + 2n\mathrm{H}_2 \rightharpoonup \mathrm{C}_n\mathrm{H}_{2n+1}\mathrm{OH} + (n - 1)\mathrm{H}_2\mathrm{O}$$

side reactions

$$n\mathrm{CO} + (2n + 1)\mathrm{H}_2 \rightharpoonup \mathrm{C}_n\mathrm{H}_{2n+2} + n\mathrm{H}_2\mathrm{O}$$

$$\mathrm{CO} + \mathrm{H}_2\mathrm{O} \rightleftharpoons \mathrm{CO}_2 + \mathrm{H}_2$$

And as a result, the separation of the ten-component system, H_2, CO, CO_2, CH_4, C_2H_6, C_3H_8, H_2O, CH_3OH, C_2H_5OH, and C_3H_7OH, becomes important in process design. Although there are much data available in some literature for the binary components of the system, little or no data exist at the conditions of interest for the CO_2–alcohol binaries, methane–alcohol binaries, and ethane–alcohol binaries. Furthermore, no multicomponent phase equilibria data exist for the above mentioned multicomponent system at any conditions.

In this work, we report on the design of a new static phase equilibrium apparatus and also report isothermal high-pressure vapor–liquid equilibrium data for the CO_2–methanol, CO_2–ethanol, CO_2–1-propanol, methane–ethanol, methane-1-propanol, ethane–ethanol, and ethane–1-propanol systems in the 313–333 K temperature range.

Experiment

Apparatus. The vapor–liquid equilibrium apparatus is shown in Figure 1 and was designed to accommodate the ten-component system. It is a static type of apparatus in which the coexisting phases are recirculated, sampled, and analyzed.

The apparatus is made up of two sections: (i) an equilibration section that consists of an equilibrium cell, 1, enclosed in an air bath, 23, at the temperature of interest and (ii) an analysis section that consists of a homogenizing system enclosed by an air bath, 24, kept at a temperature much greater than the equilibrium temperature. The air bath of each section was controlled to ±0.1 K by a Pt sensor PID controller (REX-C1000, REK Co.). The temperature in the equilibrium cell could be measured by a platinum resistance probe (Shimaden SD-10) with digital readout to ±0.1 K. Pressure in the equilibrium cell could be measured by either a Bourdon gauge (GP35, Nagano Co.), 0–250 kg/cm^2 marked in 0.5 divisions, or a $4^1/_2$ digital gauge, 0–200 kg/cm^2 (GC-11, Nagano).

Equilibrium Cell. The equilibrium cell consisted of a two-piece autoclave with a titanium delta-ring and was designed to carry a maximum pressure of 25 MPa at 453 K. Three pairs of diametrically opposed windows of 12-mm o.d. with Vespal gaskets (Du Pont Co.) allowed viewing of the sample and liquid level. Further details of the cell design are given in Figure 2.

Sampling Valves. Details of the sampling valves are given in Figures 3 and 4. Each was constructed from 316-type stainless steel and consisted of two pairs of two-way valves placed at 90° angles from each other and two holes in the body that allowed for heating with cartridge heaters. The internal volume of the liquid sampler was 0.75 cm^3. The internal volume of the vapor sampler could be varied from 1 to 10 cm^3 by manually changing a stainless steel insert.

Chromatograph Arrangement. The gas chromatographs (Shimadzu GC-8A) were fitted with thermal conductivity detec-

0021-9568/90/1735-0063$02.50/0 © 1990 American Chemical Society

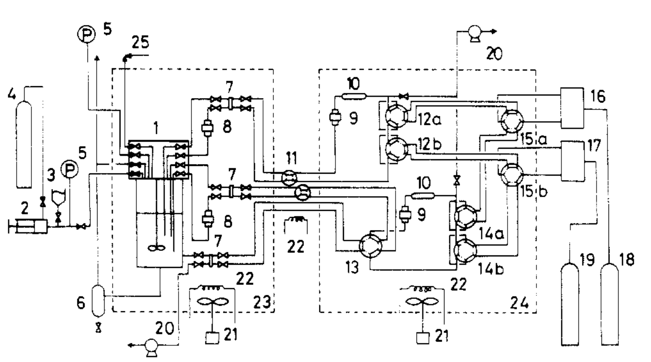

Figure 1. Schematic diagram of apparatus: 1, equilibrium cell; 2, charge pump; 3, liquid supply; 4, gas-sample cylinder; 5, pressure gauge; 6, drain tank; 7, sampler; 8-9, magnetic pump; 10, flash tank; 11, four-way valve; 12-15, six-way valve; 16 and 17, gas chromatographs (GC-1, GC-2, respectively); 18, Ar-gas cylinder; 19, He-gas cylinder; 20, vacuum pump; 21, stirrer; 22, heater; 23 and 24, air baths; 25, safety valve.

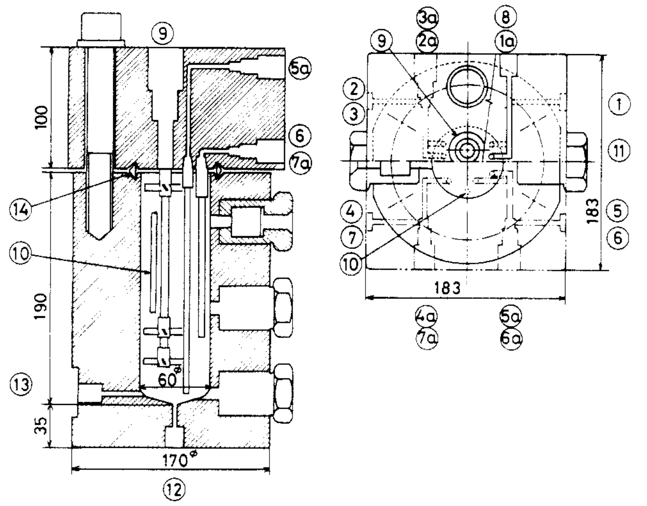

Figure 2. Equilibrium cell: 1, sample inlet; 2, pressure-gauge tap; 3, vent tap; 4, gas outlet; 5, liquid outlet; 6, gas inlet; 7, liquid inlet; 8, safty-valve tap; 9, magnetic pump; 10, thermowell; 11, circular window; 12, drain outlet; 13, liquid outlet; 14, titanium delta-ring. (The "a" denotes a valve seat.)

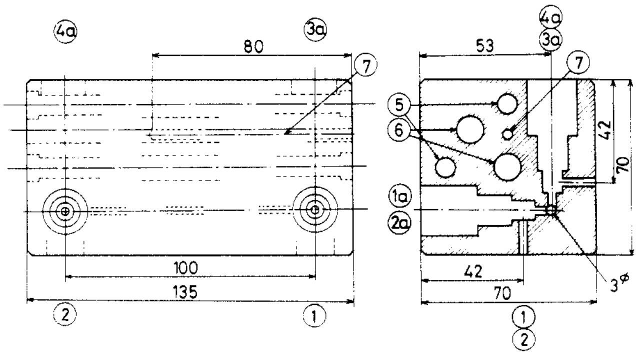

Figure 3. Liquid-phase sampling valve: 1, inlet (cell side); 2, outlet (cell side); 3, inlet (flash-tank side); 4, outlet (flash-tank side); 5, cooling air hole; 6, cartridge heater hole; 7, thermowell. (The "a" denotes a valve seat.)

tors (TCD) and reporting integrators (Shimadzu Chromatopac C-R3A). In Figure 1, six-way valves, 15a and 15b, determine whether GC-1, 16, and GC-2, 17 analyze the vapor or liquid phase sample. Manipulation of six-way valves 12a and 12b or valves 14a and 14b brings one sample of vapor or liquid to each of the chromatographs.

The gas chromatography column arrangement shown in Figure 5 was designed to analyze the ten-component system.

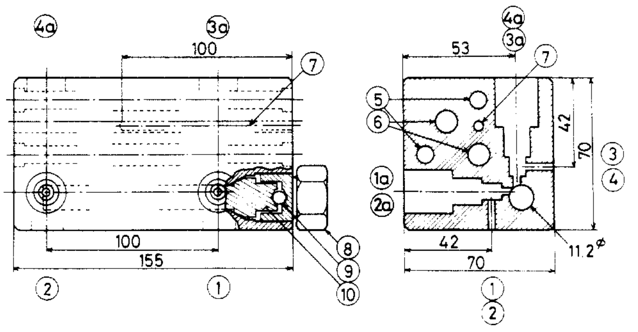

Figure 4. Gas-phase sampling valve: 1, inlet (cell side); 2, outlet (cell side); 3, inlet (flash-tank side); 4, outlet (flash-tank side); 5, cooling air hole; 6, cartridge heater hole; 7, thermowell; 8, plug; 9, metal ball; 10, insert. (The "a" denotes a valve seat.)

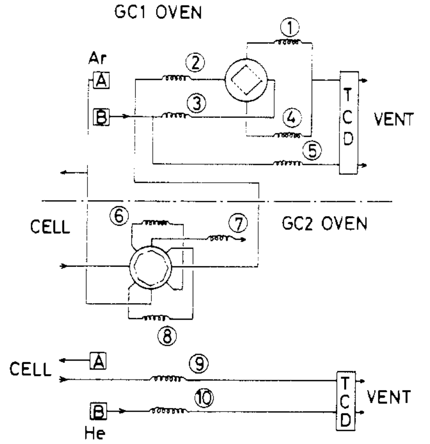

Figure 5. Schematic diagram of gas chromatograph columns: 1, molecular sieve-13X (3 m); 2, Porapak-N (1 m); 3, Porapak-N (2 m); 4, empty (7 m) + Porapak-Q (3 m); 5, Shimalite-Q (1 m); 6, Porapak-N (1 m); 7, Shimalite-Q (2 m); 8, Porapak-N (1 m); 9, polyethylene glycol-6000 (2 m) + poly(phenyl ether) (5 rings) (1 m); 10, polyethylene glycol-6000 (2 m).

It also can be used to analyze any combination mixtures of the previously mentioned ten components. Argon carrier gas was used for the analysis of gas components, H_2, CO, CO_2, CH_4, C_2H_6, and C_3H_8, while helium gas was used for liquid components, H_2O, CH_3OH, C_2H_5OH, and C_3H_7OH.

Calibration. The Pt resistance temperature probe (Shimaden SD-10) was calibrated against a Hewlett-Packard 2804A quartz thermometer accurate to ±0.025 K. The final accuracy of the temperature measurements is estimated to be ±0.2 K due to some difficulties with vapor condensation explained later. Both Bourdon and digital pressure gauges were checked with a dead-weight tester from Nagano. The final accuracy of the pressure measurements is estimated to be ±0.02 MPa.

Gas chromatography calibration was made by making plots of peak area versus mole number. For the case of liquid samples, microsyringes were weighed on a $5^1/_2$ digital Mettler AE-163 balance before and after injection. Gaseous samples were loaded into volume-calibrated tubes at a measured temperature and desired pressure. The number of moles could be estimated from the virial equation of state with the values of Dymond and Smith (*1*). Accuracy of the gas and liquid composition by this procedure is estimated to be 1% and 3%, respectively.

Since two samples were required for both gas and liquid analysis, the volume ratios of loops 12a/12b and 14a/14b in Figure 1 were measured with N_2 gas. These ratios were then applied to the peak area as a correction. Three analyses were made for each sample, and only the data with a maximum reproducibility of 0.5% were used.

Table I. List of Materials

component	purity, %	maker
CO_2	99.99	Showa Tansan Co., Ltd
methane	99.95	Nippon Sanso Co., Ltd.
ethane	99.7	Nippon Sanso Co., Ltd.
propane	99.9	Takachiho Kagakukogyo Co., Ltd.
methanol	99.6	Wako Pure Chem. Ind. Co., Ltd.
ethanol	99.5	Wako Pure Chem. Ind. Co., Ltd.
1-propanol	99.5	Wako Pure Chem. Ind. Co., Ltd.

Table II. Vapor–Liquid Equilibria of the Carbon Dioxide (1)–Methanol (2) System

P, MPa	$x(1)$	$y(1)$	P, MPa	$x(1)$	$y(1)$
313.4 K					
0.683	0.031	0.944	4.910	0.283	0.986
1.126	0.055	0.965	6.954	0.482	0.984
2.145	0.111	0.980	7.400	0.552	0.983
2.986	0.163	0.983	7.713	0.616	0.981

Table III. Vapor–Liquid Equilibria of the Carbon Dioxide (1)–Ethanol (2) System

P, MPa	$x(1)$	$y(1)$	P, MPa	$x(1)$	$y(1)$
313.4 K					
0.514	0.026	0.960	5.059	0.305	0.991
1.155	0.064	0.981	6.022	0.398	0.991
2.061	0.111	0.988	7.102	0.552	0.987
3.020	0.166	0.991	7.437	0.638	0.987
3.925	0.226	0.991	7.906	0.873	0.981
333.4 K					
0.544	0.020	0.905	7.529	0.372	0.979
0.991	0.038	0.947	9.024	0.494	0.972
2.110	0.088	0.972	9.949	0.610	0.954
3.030	0.129	0.978	10.518	0.726	0.934
4.043	0.169	0.981	10.580	0.763	0.923
4.993	0.217	0.982	10.654	0.817	0.908
6.094	0.278	0.981			

Safety Precautions. Because of high pressures and because some of the system components are toxic or explosive, a safety valve and rupture disks were placed in both high- and low-pressure sections. The entire area was enclosed in a hood that was continuously monitored by a CO/combustible-gas detector that could automatically turn on a 450-W, 110 m^3/min blower.

Procedure

Materials. The materials and their source and purity are given in Table I. Besides the liquids being degassed in the cell, substances were used without further purification.

Experiment. Each experiment began by evacuation of the apparatus overnight to a pressure of below 0.1 Pa. Materials were fed into the cell through a 300-cm^3 high-pressure piston pump until the desired pressure was achieved. Once the cell was loaded, the vapor and liquid phases were recirculated through the sampling valves by pneumatically controlled magnetic pumps and were vigorously stirred by the magnetic coupled stirrer.

After 8 h, the magnetic pumps and stirrer were cut off and the system was allowed to settle. Samples were isolated in the sampling valves and flashed to the low-pressure section, and all line heaters and sampling valve heaters were activated. Low-pressure magnetic pumps of 700 cm^3 in volume were used for stirring action, and 300-cm^3 surge tanks provided additional system volume. Pressure of the analysis section could be monitored by two Bourdon-tube gauges that could be valved off from the system. Initially, the analysis system was kept at 498 K, but it was found that 423 K was adequate to ensure that the samples were completely vaporized.

Once the sample was homogenized, the six-way valves could be manipulated as explained in the previous section such that the samples could be analyzed by gas chromatographs.

Table IV. Vapor–Liquid Equilibria of the Carbon Dioxide (1)–1-Propanol (2) System

P, MPa	$x(1)$	$y(1)$	P, MPa	$x(1)$	$y(1)$
313.4 K					
0.518	0.037	0.983	6.035	0.435	0.995
1.171	0.087	0.993	6.979	0.529	0.993
2.600	0.181	0.996	7.580	0.668	0.989
4.062	0.292	0.996	7.999	0.908	0.987
5.076	0.356	0.996	8.179	0.961	0.985
333.4 K					
0.668	0.031	0.969	7.870	0.428	0.988
1.163	0.054	0.980	9.574	0.586	0.978
3.118	0.151	0.990	10.414	0.705	0.960
4.966	0.246	0.991	10.822	0.812	0.942
6.081	0.309	0.991			

Table V. Vapor–Liquid Equilibria in the Methane (1)–Ethanol (2) System

P, MPa	$x(1)$	$y(1)$	P, MPa	$x(1)$	$y(1)$
313.4 K					
1.808	0.021	0.989	7.254	0.080	0.995
3.662	0.041	0.993	10.073	0.107	0.995
5.052	0.057	0.994			
333.4 K					
2.594	0.028	0.977	8.089	0.083	0.988
4.460	0.047	0.985	10.464	0.105	0.989
6.311	0.066	0.987			

Table VI. Vapor–Liquid Equilibria of the Methane (1)–1-Propanol (2) System

P, MPa	$x(1)$	$y(1)$	P, MPa	$x(1)$	$y(1)$
313.4 K					
2.165	0.036	0.996	8.082	0.116	0.998
3.740	0.059	0.997	10.079	0.141	0.998
5.761[a]	0.094	0.998			
333.4 K					
1.410	0.020	0.985	7.026	0.092	0.994
3.205	0.044	0.992	10.197	0.130	0.994
5.126	0.069	0.994			

[a] The experimental error of the datum at 5.761 MPa was large in comparison with other data.

Table VII. Vapor–Liquid Equilbria of the Ethane (1)–Ethanol (2) System

P, MPa	$x(1)$	$y(1)$	P, MPa	$x(1)$	$y(1)$
313.4 K					
1.365	0.078	0.984	5.117	0.473	0.988
3.225	0.214	0.992	5.414	0.602	0.968
4.216	0.316	0.992			
333.4 K					
1.307	0.057	0.958	7.177	0.466	0.936
2.655	0.122	0.977	7.481	0.508	0.919
4.256	0.214	0.981	7.700	0.535	0.904
5.188	0.279	0.981	7.897	0.567	0.882
6.504	0.395	0.975			

Table VIII. Vapor–Liquid Equilibria in the Ethane (1)–1-Propanol (2) System

P, MPa	$x(1)$	$y(1)$	P, MPa	$x(1)$	$y(1)$
313.4 K					
1.347	0.106	0.994	4.489	0.426	0.996
2.653	0.218	0.996	5.111	0.547	0.994
3.698	0.321	0.996			
333.4 K					
1.356	0.080	0.984	5.036	0.335	0.991
2.811	0.174	0.990	5.967	0.421	0.989
4.216	0.273	0.991	6.742	0.503	0.971

Some problems occurred in the recirculation of the equilibrium vapor phase. Because the liquid samples tended to con-

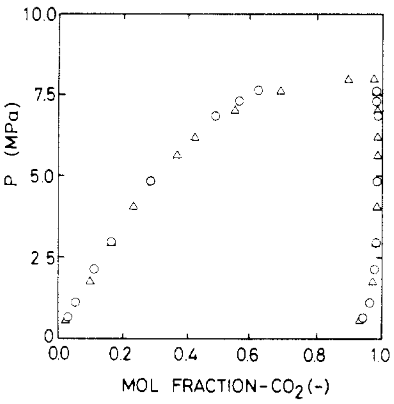

Figure 6. Vapor-liquid equilibria for the CO_2-CH_3OH system: O, this work at 313.4 K; △, Ohgaki et al. at 313.2 K.

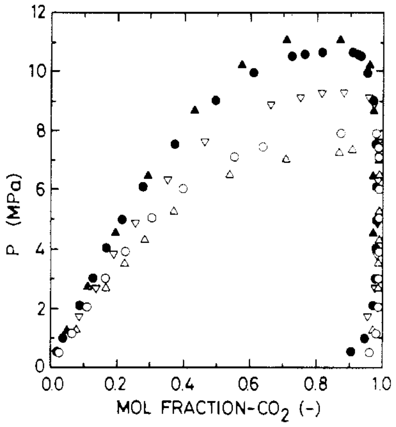

Figure 7. Vapor-liquid equilibria for the CO_2-C_2H_5OH system: O, this work at 313.4 K; ●, this work at 333.4 K; △, Panagiotopoulos et al. at 308.1 K; ▽, Panagiotopoulos et al. at 323.1 K; ▲, Panagiotopoulos et al. at 338.1 K.

dense in the sampler, the sampler had to be gently heated to a temperature slightly higher than the equilibrium cell temperature. This temperature was typically 2-3 K higher than the cell temperature but never exceeded 5 K. The change in the cell temperature and of the sampling tubing due to this slight heating was determined to be negligible.

Experimental Results and Discussion

Data obtained are shown in Tables II-VIII and Figures 6-8. We began our study with the CO_2-methanol system to confirm our apparatus and procedure because this system has been well studied. The P-x-y data shown in Table II and plotted in Figure 6 show good agreement with the data of Ohgaki and Katayama (*3*).

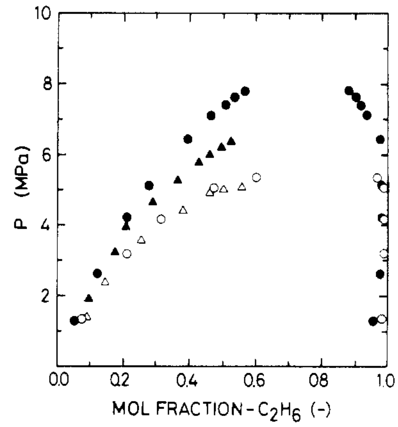

Figure 8. Vapor-liquid equilibria for the C_2H_6-C_2H_5OH system: O, this work at 313.4 K; ●, this work at 333.4 K; △, McHugh et al. at 310.3 K; ▲, McHugh et al. at 323.2 K.

P-x-y data for the CO_2-ethanol system at 313.4 and 333.4 K are given in Table III and plotted in Figure 7 with the data of Panagiotopolous and Reid (*4*).

P-x-y data for the CO_2-1-propanol system are given in Table IV. For this system, there are no reported data that we know of. All of the CO_2-alcohol systems that we studied showed a similar P-T-x-y envelope shape.

The methane-ethanol, methane-1-propanol, ethane-ethanol, ethane-1-propanol systems data are given in Tables V-VIII, respectively. Both ethane and CO_2 showed a higher solubility in the alcohols than methane as would be expected in view of their critical temperatures. Data for the ethane-ethanol system are shown in Figure 8 along with the data of McHugh et al. (*2*).

Literature Cited

(1) Dymond, J. H.; Smith, E. B. *The Virial Coefficients of Gases*; Oxford University Press: Oxford, 1969.

(2) McHugh, M. A.; Mallet, M. W.; Kohn, J. P. In *Chemical Engineering at Supercritical Fluid Condition*; Paulaitis, M. E., Penninger, J. M. L., Gray, R. D., Davidson, P., Eds.; Ann Arbor Science: Stoneham, MA, 1983; Chapter 5.

(3) Ohgaki, K.; Katayama, T. *J. Chem. Eng. Data* **1976**, *21*, 53.

(4) Panagiotopoulos, A. Z.; Reid, R. C. In *Equations of State*; Chao, K. C., Robinson, R. L., Eds.; ACS Symposium Series 300; American Chemical Society: Washington, DC, 1986; p 571.

Received for review July 18, 1988. Accepted October 2, 1989.